Mining of Mineral Deposits
Volume 19 (2025), Issue 4, 40-52

https://doi.org/10.33271/mining19.04.040

Numerical study of the influence of the angle of inclination and resistance of the mine workings on the formation of air flows during a fire

Dmytro Brovko [1], Roman Makareiko [2], Serhiy Sakhno [1*], Lyudmyla Yanova [1], Olena Pischikova [1]

[1] *Kryvyi Rih National University, Kryvyi Rih, Ukraine*
[2] *State Militarized Mine-Rescue (Rescue) Squad Public Service of Ukraine for Emergencies, Kryvyi Rih, Ukraine*
**Corresponding author: e-mail sakhno.serhiy@knu.edu.ua*

Abstract

Purpose. This study aimed to investigate the influence of the inclination angle and aerodynamic resistance of mine workings on airflow dynamics during a fire.

Methods. A model based on the ArcelorMittal Kryvyi Rih open-pit mine ventilation network, with a 15-degree inclination angle, was employed to analyze airflow patterns during fire conditions. Airflow during the fire was modeled using the Ventsim program. Correlation and multiple regression analyses were used to identify the effects of working inclination and resistance on the nature of airflow.

Findings. Correlation analysis revealed a strong negative correlation between linear resistance and airflow volume in the "cold" and "hot" areas. The angle of inclination and linear resistance have different effects on airflow volume, depending on the site location relative to the fire center. The main factor affecting airflow in the longitudinal sections is the linear resistance. The effect of the angle of inclination was most noticeable in the "hot" areas. The results show that the crosscut section located immediately behind the section with the fire center is mainly influenced by the "cold" longitudinal sections found above and below and the "hot" section with the fire center. Simultaneously, an increase in the inclination angle, together with an increase in the resistance of the working face, increases the influence of the area with the fire center. In the case of a decrease in the inclination and resistance of the working face, the value of the "cold" adjacent workings increases.

Originality. This study provides a novel analysis of airflow dynamics in inclined mine workings, particularly during fire incidents. This study contributes to a better understanding of the mechanisms of jet direction change and combustion product propagation during fires in inclined workings.

Practical implications. The findings of this study enable the prediction of fire occurrence, identification of areas most susceptible to fire, and formulation of best strategies for fire suppression under specific conditions.

Keywords: *underground fire, mine safety, ventilation network, mining, Computational Fluid Dynamics*

1. Introduction

1.1. The problem formulation

The mining industry plays a key role in the global economy by providing essential raw materials for modern society. From smartphones and computers to cars and buildings, virtually every product we use is based on minerals extracted from the Earth's interior. Mining generates significant revenue for countries, creating jobs and supporting local communities. The manufacturing industry depends on minerals to produce machinery, tools and components.

The mining sector is a key driver of Ukraine's economic growth. Ukraine was the tenth largest iron ore producer in the world in 2023 [1]. With a strong raw material base of iron ore, Ukraine plays a key role in the mining and metallurgy industries. This raw material base offers significant potential for the development of the mining and related industries. However, efficient utilization and addressing environmental and technological challenges are crucial for its success. Despite its economic advantages, the mining industry in Ukraine faces critical safety issues, including mine fires, which not only pose risks to human life but also have serious environmental consequences for the surrounding areas. Fires in underground mines are among the most severe emergencies. Mine fires create smoke and high concentrations of toxic gases, as well as significant changes in the microclimatic conditions of the mine workings. Fires in inclined mine workings can interfere with ventilation in both isolated and large areas of the minefield, leading to the overturning of ventilation jets, creation of recirculation circuits, and convective movements of fire gases, as well as contamination of working areas with fresh airflow and a decrease in

Received: 12 June 2025. Accepted: 23 October 2025. Available online: 30 December 2025

Mining of Mineral Deposits. ISSN 2415-3443 (Online) | ISSN 2415-3435 (Print)

air velocity [2]. Such conditions complicate the management and elimination of accidents and their consequences, potentially resulting in human casualties.

Airflow formation analysis during mine fires is a critical research area for several compelling reasons.

1. Mine fires pose an immediate risk to miners' health and safety. Understanding airflow patterns can facilitate the prediction of the spread of smoke and toxic gases, thus improving evacuation techniques and limiting exposure to hazardous conditions.

2. Efficient ventilation is essential in mines to control the spread of fires and to mitigate their effects. By analyzing airflow dynamics, more effective strategies can be developed to extinguish and locate fires.

3. Mine fires can release significant amounts of pollutants and greenhouse gases into the atmosphere. A detailed understanding of airflows can help model and reduce these emissions, thereby reducing their impact on air quality and climate change.

4. Mines often contain significant amounts of valuable resources and infrastructure components. Knowledge of airflow can help design the best protective measures to prevent grave damage during fires.

5. Understanding the conditions that lead to mine fires can provide a basis for preventive strategies. In-depth studies of airflows can lead to improved monitoring systems, thereby increasing the ability to detect and respond to these events early.

Many countries have regulations related to mining safety and environmental protection. Research on airflow during fires can help mining companies comply with these regulations and ensure safer operations. A deeper understanding of airflow can contribute to the development of advanced simulation models and technologies that will facilitate both prediction and response maneuvers in the event of a mine fire. Thus, studying the formation of airflows during mine fires is important for protecting human life, preserving the environment, and improving safety and operational protocols in the mining sector.

1.2. Analysis of research and publications

Studies on airflow dynamics during mine fires have revealed complex patterns and critical safety considerations. Studies have shown that mine fires can profoundly alter ventilation flows, potentially leading to unsafe conditions [2], [3]. The heat generated by a fire causes thermal pressure that affects the mine ventilation system, thereby disrupting airflow. As the fire intensifies, the air movement in the side passages may weaken, stagnate, or change direction [2]. This phenomenon, known as airflow velocity sign reversal, occurs in blind drifts, unused workings, and underground fires [4]. A "heat ball", a concentrated area of high temperature, can cause airflow to reverse in inclined mines. This phenomenon is closely related to the design of the mine and airflow characteristics [3]. In particular, low-density fire gases tend to accumulate on the mine ceiling and gradually mix linearly with air.

When the air velocity reaches 0.67-0.7 m/s, fire gas flows can counteract the ventilation flow without mixing, creating a bifurcation effect [5]. This behavior significantly affects the dispersion of smoke and toxic gases in mine ventilation systems. Therefore, understanding the development of airflow during mine fires is crucial for developing effective fire-prevention and management strategies. Research emphasizes the need to consider thermal effects, mine design, and ventilation characteristics when predicting and controlling fire-induced airflow alterations. While understanding the critical impact of mine fires on airflow dynamics, it is also important to consider how the physical structure of the mine, such as the slope angle and aerodynamic drag, further complicates these dynamics. Airflow is greatly influenced by the angle of the workings.

A study [6] investigated the effect of tunnel slope on the critical velocity for density and fire plumes in ventilated tunnels, illustrating that the slope has a profound effect on the dynamics of airflow during fires. Another study on the smoke back-layering length and inlet air velocity of fires in inclined tunnels under natural ventilation with a vertical shaft [7] emphasized the effect of tunnel slope on the temperature distribution in the mine and tunnel, the length of the smoke layer, and the increase in air velocity at the tunnel inlet, which was shown to increase exponentially with increasing tunnel slope.

The study conducted by [8] presents theoretical and experimental results on the characteristics of airflow in inclined tunnels, emphasizing that stratification in such environments reduces the flow rate. The study [9] investigates the dependence of wind pressure generated by a fire on the increase in the tunnel angle. In addition, aerodynamic drag significantly affects airflow dynamics.

A study [10] indicates that in a mine ventilation system, the pressure caused by a fire interacts with thermal resistance, directly disturbing the airflow in the ventilation system, and presents a methodology for assessing the sensitivity of primary airflow directions in ventilation subnetworks to changes in aerodynamic drag and air density in mine workings. The authors formulated an equation to assess the sensitivity of the direction of primary air flows in a subnetwork by quantifying the degree of dependence of the main subnetwork flows on changes in the volume of airflow in specific workings caused by changes in aerodynamic drag or air density in other workings of the network. The authors emphasize that the use of modern numerical models to analyze the distribution of air flows in underground workings provides significant advantages, for example, when assessing the level of safety or operational risk.

Most researchers have investigated the effects of individual variables, such as slope angle and airflow resistance, without considering their combined effects. Moreover, the effect of the angle of inclination on the formation of air flows has been studied in tunnels without branches or connections. In contrast, the study [11] considered the formation of air flows in inclined conveyor workings consisting of two parallel longitudinal sections and seven crosscut sections. Fluent CFD modeling was used to evaluate the factors affecting airflow during mine-fire scenarios. However, the results were only applicable to a single slope angle and constant resistance parameters in specific mine sections. The absence of scientific papers on the dynamics of airflow at variable inclination angles and the aerodynamic drag of mine workings proves the importance of research in this area.

Conducting physical experiments under such conditions is difficult and costly because it is almost impossible to find several geometrically identical mine workings that differ only in their angles of inclination or airflow resistance. Therefore, CFD modeling is recommended for such analyses. CFD modeling provides a detailed understanding of the

structure of air flows, temperature distribution, and dispersion of pollutants in the mine works. It offers higher accuracy and visualization capabilities than traditional methods, allowing for better analysis and optimization of ventilation systems [12]-[14].

Well-known software tools, such as Ventsim, Minevent, and Ventpac, are used to model airflow in mine ventilation networks. In this study, we used Ventsim software to investigate the effects of slope angle and rock resistance on airflow formation. Developed by the Howden Group of Australia, Ventsim facilitates the accurate and efficient modeling of both the current state of mine ventilation and its design and long-term planning. Global evidence supports the effective use of Ventsim for modeling mine ventilation networks. The comprehensive application of Ventsim in this field has been thoroughly documented in [15]. The studies demonstrated a strong correlation between the calculated and actual airflow parameters in mine ventilation systems that are applicable to standard and emergency conditions.

Fires in underground mines are considered one of the most dangerous emergencies. Such fires emit smoke and elevated levels of toxic gases that profoundly alter the microclimate of the mine environment. Analyzing airflow during such fires is essential for protecting human life, preserving the environment, and improving safety and operational protocols in the mining sector. Studies have shown that mine fires can significantly alter ventilation dynamics, leading to hazardous conditions. The behavior of airflow during a fire is significantly influenced by the physical characteristics of the mine, including its slope and aerodynamic drag. To date, no study has thoroughly examined how changes in slope and drag affect airflow in mines. Given the impracticality of finding several geometrically similar workings that differ only in slope or airflow resistance, computational fluid dynamics (CFD) modeling is recommended. Ventsim is recognized as the optimal software package for such analyses. Based on the above, the aim of this study was to investigate the influence of the angle of inclination and aerodynamic resistance of mine workings on the dynamics of airflow formation during a fire using the Ventsim software package.

2. Materials and methods

To study the influence of the angle of inclination and resistance of the workings on the nature of air flows during a fire, we used the configuration of an inclined conveyor working in the ArcelorMittal Kryvyi Rih open-pit mine with an actual slope of 15°.

The model verification was carried out by simulating the airflow of the existing mine using Ventsim, taking into account the actual cross-sections and aerodynamic resistances of the sections, as well as the actual temperatures, velocities, and volumes of air supplied to the working area. All air and mine parameters were obtained through field studies. The results of these measurements are presented in Tables 2 and 5 of work [11]. The model created in Ventsim demonstrated a high degree of agreement between the measured and simulated flow parameters. Deviations in parameter values did not exceed 3%. The high reliability of the results generated by the Ventsim model made it possible to use this software package for the research discussed in this article.

To ensure the purity of the experiment, the mathematical model of the workings was simplified by removing elements that did not affect the formation of air flows. Furthermore, the model varied the angles of inclination of the longitudinal sections of the working face (0°, 5°, 10° and 15°) and changed the linear resistances of the sections (R/100 = 0.002, 0.01, and 0.05 Ns^2/m^8). Thus, a total of 12 combinations of dip angle and face resistance were considered. The results of the experimental planning are presented in Table 1.

Table 1. Combinations of linear resistance values and inclination angles of the working face used to study the influence of these factors on the formation of air flows on the working face

Factor_1: R/100, Ns^2/m^8	Factor_2: degree, (°)
0.002	0
0.002	5
0.002	10
0.002	15
0.01	0
0.01	5
0.01	10
0.01	15
0.05	0
0.05	5
0.05	10
0.05	15

The general geometric scheme of the mathematical model of the mine is shown in Figure 1, and the geometric and aerological parameters are listed in Table 2.

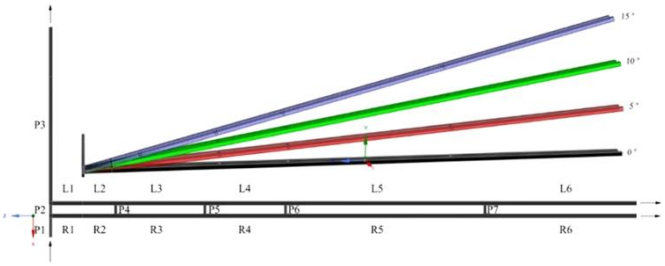

Figure 1. Mathematical model of the working at different inclination angles

Table 2. Geometric and aerodynamic parameters of working areas

Section	Length, m	Cross-sectional area, m^2	Type of section resistance	Resistance, Ns^2/m^8	Angle of inclination
P1	20.0	9.214	Total	0.03284	0
P2	12.0	9.214	Total	0.00031	0
P3	168.0	14.039	Total	1.53654	0
P4	12.0	9.214	Linear/100	Factor_1	0
P5	12.0	9.214	Linear/100	Factor_1	0
P6	12.0	9.214	Linear/100	Factor_1	0
P7	12.0	9.214	Linear/100	Factor_1	0
R1	31.0	19.875	Linear/100	Factor_1	Factor_2
R2	31.0	19.875	Linear/100	Factor_1	Factor_2
R3	85.0	19.875	Linear/100	Factor_1	Factor_2
R4	77.0	19.875	Linear/100	Factor_1	Factor_2
R5	190.0	19.875	Linear/100	Factor_1	Factor_2
R6	208.0	19.875	Linear/100	Factor_1	Factor_2
L1	31.0	19.875	Linear/100	Factor_1	Factor_2
L2	31.0	19.875	Linear/100	Factor_1	Factor_2
L3	85.0	19.875	Linear/100	Factor_1	Factor_2
L4	77.0	19.875	Linear/100	Factor_1	Factor_2
L5	190.0	19.875	Linear/100	Factor_1	Factor_2
L6	208.0	19.875	Linear/100	Factor_1	Factor_2

Airflow during the fire was modeled using the Ventsim program. The longitudinal workings are conventionally divided into the right branch with the index of sections R and the left branch with the index of sections L. Because the fire was located in section R3, this section and all sections of the right branch are referred to in the text as "hot" sections or sections of the "hot" branch. In contrast, plots on the left branch may be referred to as "cold" plots or "cold branch" plots in the text. All crosscut sections are labeled with the P index.

The center of the fire was the rubber belt of the conveyor. The fire simulation included three time stages:

1. The first stage is Fire Growing, during which the amount of rubber burned varies from 0 to 982 kg/h. This stage lasted for 20 min (1200 s).

2. The second stage is Fire Stabilizes, in which the amount of rubber that burns is unchanged and equals 982 kg/h. The duration of this stage was 20 min (1200 s).

3. The third stage is Fire Degradation, in which the amount of rubber that burns is reduced from 982 to 0 kg/h. This stage lasted for 20 min (1200 s).

The rubber burning rate of 982 kg/hour corresponds to a heat output of 9 MW. The modeling was performed without any restrictions on the amount of oxygen.

During the course of modeling, Dynamic Monitors were installed on the longitudinal and crosscut sections of the inclined part of the working face, which made it possible to control the airflow parameters over time. The values of airflow Q (m^3/s), air flow velocity V (m/s), air density ρ (kg/m^3), air temperature T (°C), and wall temperature t (°C) were recorded for each section. The readings were recorded at 10 s intervals. Simultaneously, the fire heat release rate (Fire HRR) (MW) was recorded.

During the simulation, air at a temperature of 20°C was supplied at a constant pressure of 96 Pa through section P1. Modeling the air supply at a constant pressure allows us to more accurately simulate the change in the airflow rate as the resistance of the workings changes. Air was considered a compressible gas. The gravity and natural draft were considered in the calculations. Magnetite with the following thermal characteristics was considered as the rock of the working face (Table 3).

Table 3. Thermal characteristics of the rock used in the modeling of the workings.

Rock-type preset	Magnetite
Conductivity, W/mC	4.41
Diffusivity, $m^2/s \cdot 10^{-6}$	2.10
Specific heat, J/kgC	600.00
Rock density, kg/m^3	3500.00

Correlation and multiple regression analyses were used to identify the effects of working inclination and resistance on the nature of airflow.

3. Results and discussion

3.1. Correlation analysis of modeling results

To identify the significance of the main factors that affect the nature of the airflow in various parts of the mine, we performed a correlation analysis of the modeling results. Because the influence of remote areas is insignificant, we simplified the calculations by conducting factor analysis separately for the lower and upper parts of the workings. The strength of the relationship between the factors was assessed using the Chaddock scale. The results of the calculations are summarized in Tables 4 and 5, respectively.

The highest (strongest) correlation between linear resistance and airflow volume was observed for sections R2, L2, and L6 (correlation coefficients were -0.80, -0.83). A smaller (noticeable) correlation (-0.6, -0.67) was observed for sections R3 and R6, respectively. A very low (weak) correlation coefficient (-0.21 to -0.31) was characteristic of areas L3, L4, and L5.

The highest (most noticeable) positive correlation coefficient between the airflow volume and angle of inclination (0.58) was found at sites R3 and R4. This parameter was slightly lower (0.51) for sites R5 and R6. The highest (most noticeable) negative correlation coefficient between the airflow volume and angle of inclination of the working face (-0.65) was found for sections L3 and L4.

The table shows that for the longitudinal sections located below the fire center, the main factor affecting the airflow volume was linear resistance. For the R2 and L2 sections, the correlation coefficients were K_{kor} = -0.804 and K_{kor} = -0.838, respectively, indicating a strong negative correlation. This indicates that the airflow volume decreased with an increase in R/100.

The values of the working angle for these sections were moderate: K_{kor} = 0.403 for R2 and K_{kor} = 0.372 for L2. For the area with a fire, the influence of the angle of the working face was significantly higher (moderate correlation, K_{kor} = 0.576), which is associated with its effect on the value of the natural draft and the presence of hot air. However, in the parallel section, the angle of inclination of the working face had a more negative value (significant correlation, K_{kor} = -0.649). This indicates that the volume of airflow decreases with increasing angle of inclination.

Table 4. Matrix of correlations between each pair of variables (Q, P/100, degree, and fire HRR). Down part

Variables	Degree	P/100	Fire HRR	R2	R3	R4	L2	L3	L4	P2	P4	P5
Degree	1.000	0.000	0.000	0.403	0.577	0.576	0.373	-0.650	-0.655	0.177	-0.631	-0.314
P/100	0.000	1.000	0.000	-0.804	-0.609	-0.593	-0.839	0.232	0.311	-0.769	0.520	0.253
Fire HRR	0.000	0.000	1.000	0.209	0.259	0.327	0.220	-0.241	-0.151	0.111	-0.242	0.181
R2	0.403	-0.804	0.209	1.000	0.935	0.926	0.956	-0.663	-0.708	0.604	-0.867	-0.370
R3	0.577	-0.609	0.259	0.935	1.000	0.992	0.843	-0.880	-0.898	0.400	-0.974	-0.425
R4	0.576	-0.593	0.327	0.926	0.992	1.000	0.849	-0.867	-0.894	0.422	-0.967	-0.456
L2	0.373	-0.839	0.220	0.956	0.843	0.849	1.000	-0.497	-0.553	0.780	-0.767	-0.312
L3	-0.650	0.232	-0.241	-0.663	-0.880	-0.867	-0.497	1.000	0.972	0.002	0.909	0.420
L4	-0.655	0.311	-0.151	-0.708	-0.898	-0.894	-0.553	0.972	1.000	-0.058	0.923	0.571
P2	0.177	-0.769	0.111	0.604	0.400	0.422	0.780	0.002	-0.058	1.000	-0.332	-0.060
P4	-0.631	0.520	-0.242	-0.867	-0.974	-0.967	-0.767	0.909	0.923	-0.332	1.000	0.351
P5	-0.314	0.253	0.181	-0.370	-0.425	-0.456	-0.312	0.420	0.571	-0.060	0.351	1.000

Table 5. Matrix of correlations between each pair of variables (Q, P/100, degree, and fire HRR). Top part

Variables	Degree	P/100	Fire/HRR	R4	R5	R6	L4	L5	L6	P5	P6	P7
Degree	1.000	0.000	0.000	0.576	0.509	0.515	-0.655	-0.247	0.380	-0.314	-0.082	0.408
P/100	0.000	1.000	0.000	-0.593	-0.532	-0.680	0.311	-0.207	-0.836	0.253	0.212	-0.179
Fire/HRR	0.000	0.000	1.000	0.327	0.212	0.225	-0.151	0.066	0.236	0.182	-0.062	0.066
R4	0.576	-0.593	0.327	1.000	0.895	0.934	-0.894	-0.194	0.885	-0.456	-0.403	0.541
R5	0.509	-0.532	0.212	0.895	1.000	0.820	-0.843	-0.539	0.787	-0.533	-0.323	0.829
R6	0.515	-0.680	0.225	0.934	0.820	1.000	-0.741	-0.013	0.934	-0.379	-0.380	0.398
L4	-0.655	0.311	-0.151	-0.894	-0.843	-0.741	1.000	0.472	-0.615	0.571	0.410	-0.649
L5	-0.247	-0.207	0.066	-0.194	-0.539	-0.013	0.472	1.000	0.078	0.424	0.061	-0.863
L6	0.380	-0.836	0.236	0.885	0.787	0.934	-0.615	0.078	1.000	-0.354	-0.284	0.386
P5	-0.314	0.253	0.182	-0.456	-0.533	-0.379	0.571	0.424	-0.354	1.000	0.030	-0.568
P6	-0.082	0.212	-0.062	-0.403	-0.323	-0.380	0.410	0.061	-0.284	0.030	1.000	-0.062
P7	0.408	-0.179	0.066	0.541	0.829	0.398	-0.649	-0.863	0.386	-0.568	-0.062	1.000

An even more significant negative correlation value was observed between the airflow volumes in the areas of "cold" (without a fire center) and "hot" (with a fire center), with a value of K_{kor} = -0.880 (strong correlation). This indicates that an increase in airflow volume in the R3 section directly affects the decrease in airflow in the L3 section, and this effect significantly exceeds that of the angle of the working face.

For the area directly behind the fire center (R4), the correlation of airflow volume with slope angle and linear resistance was lower than that for the area with the fire center, but the airflow volume for R4 was significantly influenced by the airflow volume of R3 (practically functional) (K_{kor} = 0.991). This indicates that the main factor affecting the airflow in the area immediately behind the fire center is the airflow volume of the area with the fire center.

For the parallel "cold" section L4, the airflow volume in the parallel "hot" section was of the greatest importance (strong) (K_{kor} = -0.894), the value of the angle of inclination of the workings (noticeable) (K_{kor} = -0.654) was less important, and the linear resistance (moderate) (K_{kor} = 0.311) was insignificant.

The influence of the previous downstream section on the airflow volume in section R5 was lower than that in the previous pair R4-R3 (strong) K_{kor} = 0.894 versus 0.991 for the pair R4-R3, which is due to the gradual cooling of the air. This phenomenon is also associated with a decrease in the influence of the angle of inclination of the working face on the airflow volume (decrease in K_{kor} from (significant) 0.576 for R4 to (significant) 0.509 for R5).

The parallel "cold" section is characterized by low correlation coefficients for both the linear resistance and slope angle. The dependence on the parallel "hot" section is also significantly lower (noticeable) (K_{kor} = 0.538) than that of the sections below. However, this section is characterized by the interdependence of air flows with the crosscut section P7 located above (strong) (K_{kor} = 0.862).

The highest upper areas connected to the atmosphere are characterized by an increase in the influence of linear resistance on the airflow volume. The influence of the angle of inclination was less. The change in airflow volume in the R6 and L6 sections occurred almost synchronously (very strong) (K_{kor} = 0.934). This is due to a decrease in air temperature and a decrease in the value of the natural draft.

Air flows in crosscut sections are formed by the difference in pressure and volume of air flows in the adjacent longwall workings. Consequently, the distributed resistance and angle of inclination of the workings indirectly affect the airflow in the faces through the adjacent longitudinal sections. Significant values of the correlation coefficients between the airflow volumes, linear resistance, and angle of inclination of the workings were found only for the P4 section located below the fire center. For the remaining failures, only a weak-to-moderate correlation was observed.

For the air flows of the P4 section, there was a strong correlation with the air flows of sites R2 and L2 and a very strong correlation with the air flows of sites R3 and L3. Section P5 was significantly influenced by the airflow of section L4 and moderately influenced by the airflow of sections R3, L3, and R4. Air flows at section P6 were significantly influenced by air flows at section L5, moderately positively influenced by air flows at section L4, and moderately negatively influenced by air flows at sections R4 and R5.

The air flows of section P7 were strongly positively affected by section R5, strongly negatively affected by section L5, and sections R6 and L6 had a moderate effect.

The tables show a weak correlation between the heat release in the fire center and the airflow in all areas. This is because these tables are calculated based on the entire dataset, and the values of air flows at one working face slope can be canceled out by values at other slopes.

In addition to the heat generated at the fire center, the temperature of the mine walls also affects airflow. As will be shown in the following, the temperature of the walls of the "hot" areas began to increase after the start of the fire, continued to increase during the period of fire stabilization, and remained high for some time even after the end of the fire. Because this study considers three stages of fire development, 15 sections of the working, three values of the linear resistance of the working, and four inclinations of the working, the complete matrix of studies of the influence of wall temperature on the value of air flows should contain at least 3×15×3×4 = 540 cells. To reduce the volume, the effect of wall temperature on air flows was considered only in longitudinal sections with R/100 = 0.01 and only at a working with a slope of 10°. The results are presented in Table 6.

The analysis of the data sample reduced to one slope angle and one resistance showed a very high positive correlation between the heat release in the fire center and the airflow in the "hot" branch of the work for the period of fire growth. A very high correlation was also observed for sites L2, L5, and L6. The sites were characterized by a high negative correlation, indicating a high influence of air flows from parallel "hot" sections. The correlation between the airflow rate and temperature of the walls was also high or very high. The exceptions were section L3, with a noticeable correlation, and section L4, with a negative moderate correlation.

Table 6. Correlation matrix between Fire HRR, the temperature of the working face walls, and the airflow in the longitudinal sections of the working face with a slope of 10 and linear resistance of 0.01

Variables	Fire HRR			T rock		
	Period					
	1*	2**	3***	1*	2**	3***
R2	0.994	-0.066	0.991	0.988	0.908	-0.984
R3	0.965	-0.560	0.975	0.870	0.502	-0.855
R4	0.969	-0.121	0.988	0.870	0.836	-0.891
R5	0.961	-0.028	0.995	0.862	0.930	-0.969
R6	0.984	-0.016	0.990	0.867	0.912	-0.972
L2	0.994	0.063	0.988	0.991	0.861	-0.991
L3	-0.873	0.378	-0.955	0.609	-0.593	0.615
L4	-0.813	0.138	-0.931	-0.393	0.224	-0.867
L5	0.949	0.002	0.991	0.946	0.896	-0.936
L6	0.989	0.001	0.991	0.916	0.884	-0.968

* Time < 1200 seconds
** 1200 ≤ Time < 2400 seconds
*** Time ≥ 2400 seconds

During the period when the fire intensity was constant, the correlation between the heat release in the fire center and the airflow in the "hot" branch of the workings was weak, except in section R3, which had a noticeable negative correlation. The correlation between the wall temperature and airflow rate in areas R2, R4-R6 was high and very high. This is because, with a constant supply of thermal energy from the fire, the walls of the "hot" areas of the workings and partially the "cold" areas continue to heat up as a result of the injection of hot air from the "hot" areas. An increase in the wall temperature led to an increase in the airflow.

During the period when the intensity of the fire decreased, all longitudinal sections were characterized by a very high correlation between the heat release in the fire center and airflow. Simultaneously, L3 and L4, which depend on parallel "hot" areas, are characterized by a negative correlation. As the intensity of the fire decreased, the airflow in these areas increased. The correlation between the wall temperature and airflow during this period for all areas except L3 was negative, high, and very high. The airflow rate decreased in the event of a gradual slowdown in the growth of the wall temperature of the sections. In section L3, the wall temperature did not change, but the airflow increased.

Correlation analysis revealed a strong negative correlation between linear resistance and airflow volume in the "cold" and "hot" areas. The angle of inclination and linear resistance have different effects on airflow volume, depending on the site location relative to the fire center. The main factor affecting airflow in the longitudinal sections is the linear resistance. The effect of the angle of inclination was most noticeable in the "hot" areas.

During the fire growth period, there was a high positive correlation between heat release and airflow in the "hot" areas, particularly at L2, L5, and L6. There was a high negative correlation between the air flows of the "cold" and "hot" areas. At a constant fire intensity, the correlation between heat generation and airflow in the "hot" areas decreased, except for area R3. The wall temperature was strongly correlated with the airflow in areas R2, R4-R6. During the reduction period of the fire intensity, the correlation between heat release and airflow increased in all areas, with a negative correlation in L3 and L4. At this stage, the temperature of the working walls affects the decrease in airflow, except for the L3 section, where the flow increases without changing the temperature of the wall.

The dynamics of airflow in the longitudinal sections directly affect the magnitude and direction of airflow in the crosscut sections. Figures 2-5 show the data characterizing the behavior of the air flows in the crosscut sections P4-P7.

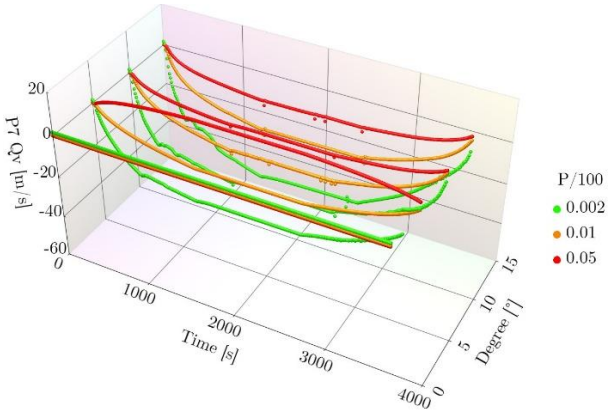

Figure 2. Influence of the resistance and inclination angle of the working face on the dynamics of air flows in the P4 area

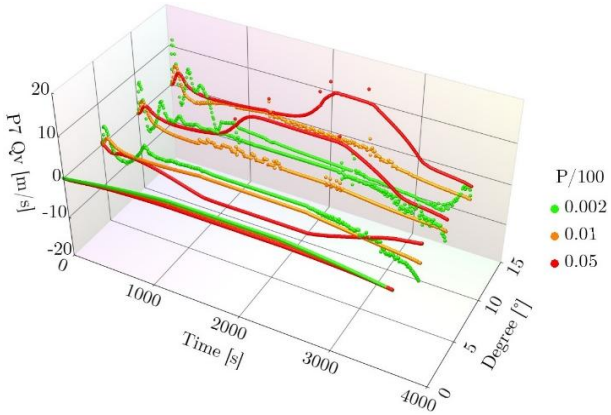

Figure 3. Influence of resistance and angle of inclination of the working face on the dynamics of air flows in the P5 area

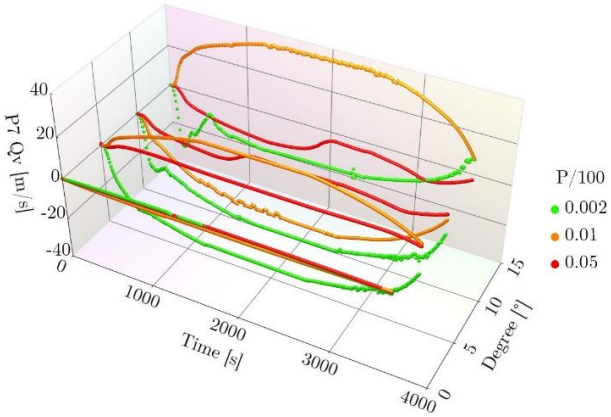

Figure 4. The effect of resistance and inclination angle of the working face on the dynamics of air flows in the P6 area

The analysis showed that the most stable air flows when HRR, linear resistance, and the angle of inclination of the working face were those of section P4 located below the fire center. The most unstable section was P5, located above the fire.

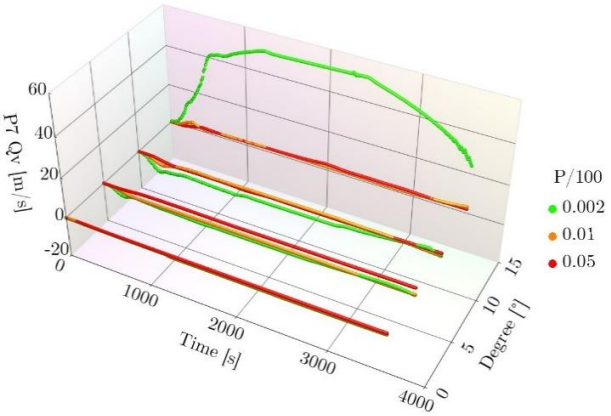

Figure 5. The effect of the resistance and angle of inclination of the working face on the dynamics of air flows in the P7 area

Owing to the limitations on the size of the article, this paper presents the results of studies related only to crosscut sections P4 and P5.

3.2. Multiple regression analysis of airflow patterns in sections P4 and P5

Multiple regression analysis allows the study of the relationships between two or more variables. In this study, the dependencies between the airflow in the crosscut workings P4 and P5 and the airflow in the adjacent longitudinal sections were identified. For section P4, these are sections R3, R4, L3, and L4. For section P5, these were R4, R5, and L4, L5, respectively. The fire HRR was considered an additional factor for both crosscut sections.

The study was conducted using a simple one-way model. All the numerical variables were included in the model. No interaction terms were included in the model. The analysis was carried out separately for each pair of combinations of degree and R/100. As a result of the calculations, the regression coefficients and standard errors were obtained, and the *R* parameter was controlled.

The degree of influence of the variables on airflow during cross-cutting work was compared using the standardized regression coefficient. Standardized regression coefficients allow for comparisons between variables with different measurement scales. The standardized regression coefficient was calculated using the following Formula:

$$b_{j,std} = b_j \left(\frac{s_{Xj}}{s_Y} \right), \quad (1)$$

where:

S_Y and S_{XJ} – the standard deviations for the dependent variable;

j – independent variable.

The standardized regression coefficients were reduced to a three-dimensional matrix, in which the rows and columns were represented by the parameters degree and R/100, and the vertical layers were the variables under study.

The results were visualized by building a 3D scatter plot for all variables simultaneously and a 3D surface plot for each variable. Because the analysis resulted in regression coefficients with positive and negative values, visualization could be performed using both the actual (sign-sensitive) and absolute values of the coefficients. To assess the impact of all variables on one graph (3D scatter plot), the absolute values of the standardized regression coefficients were used. When constructing the influence surfaces for individual parameters, values were used, considering their signs.

The impact of the Fire HRR and the dynamics of air flows in adjacent areas on the crosscut section P4 can be assessed using the summary 3D Scatter Plot (Fig. 6).

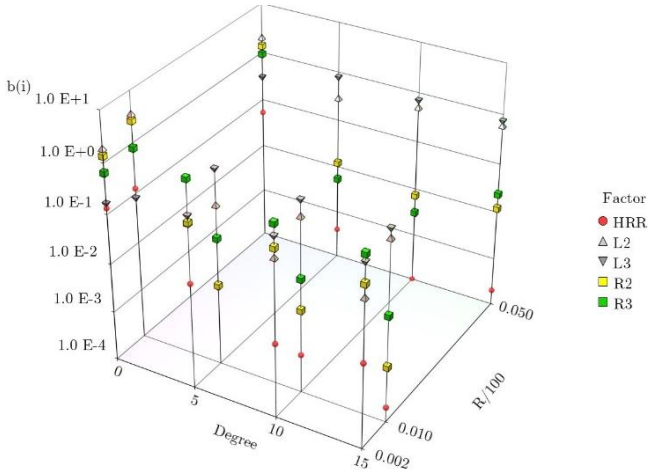

Figure 6. 3D scatter plot of the multiple regression coefficients b(i) of the variables R2, R3, L2, L3 HRR for section P4 at variable inclination angles and workings resistance

In the horizontal workings (degree = 0), the airflow pattern in the P4 section was mainly influenced by the airflow in the downstream "cold" section L2. Simultaneously, the highest value of the regression coefficient ($b(i)$ = -3.68) was recorded for the linear resistance, R/100 = 0.01. For linear resistances R/100 = 0.002 and R/100 = 0.05, the regression coefficients were -1.94 and -2.08, respectively. The second most influential factor was airflow in the "hot" sections below R2. For resistances of 0.002, 0.01, and 0.05, the regression coefficients were 1.38, 2.67, and 1.37, respectively. The degree of influence of the longitudinal sections located above and the HRR was much lower. The results obtained allow us to conclude that, in the absence of a working slope, only the airflow of the crosscut sections located below the fire center affects the dynamics of airflow.

At a slope 5° (degree = 5), the airflow pattern in section P4 at a low linear resistance of R/100 = 0.002 is mainly influenced by the airflow in the section with the fire center R3, and at resistances of 0.01 and 0.05, the airflow in the "cold" section L3 located above (L3 by 0.002 and 0.05 with a plus and 0.01 with a minus). At low resistance (R/100 = 0.002), the second most influential factor was the airflow in the L3 section, and at higher resistance, it was in the L2 section. Simultaneously, the influence of airflow in the R3 section was significantly reduced.

Similar degrees of influence of the variables were observed at slope 10 and 15°. Therefore, in the presence of a working slope, the crosscut sections (failures) located below the fire center mainly influence the dynamics of the air flows in the air flows located above the longitudinal sections. Simultaneously, if the resistance of the mine is low, the area with the fire center has the main influence, and if the resistance increases, the airflow in the cold face L3 parallel to the fire center and the second most influential cold face L2 located below the fire center has a greater impact.

When analyzing the standardized regression coefficients of the variables considered, the direct impact of the HRR on

the dynamics of the air flows at section P4 was noticeably small. However, because this variable affects air flows in the longitudinal sections, we can discuss the indirect influence of HRR on air flows in P4. The 3D surface plot (Fig. 7), which shows the value of $b(i)$ for HRR at different values of K/100 and degree, shows that the greatest direct influence of HRR on the airflow pattern at the P4 section is observed in the absence of a working slope and low values of linear resistances. When the ratio R/100 is equal to 0.01 and the degree is 0, the regression coefficient $b(i)$ for HRR is determined to be 0.13. When the resistance of the workings increased and the angle of inclination increased, the influence of HRR on the nature of the airflow in the P4 section decreased sharply.

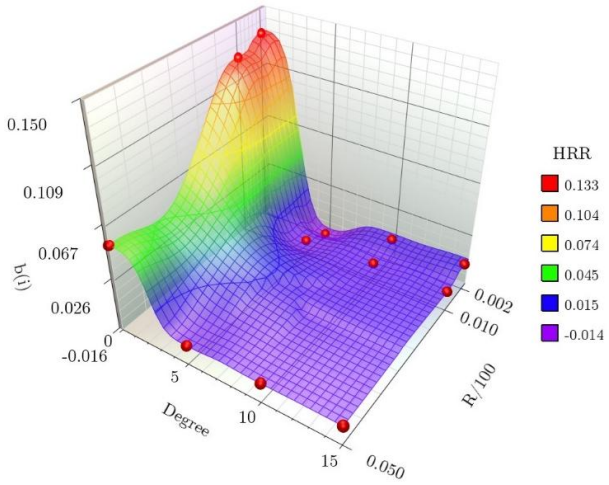

Figure 7. 3D surface plot of the multiple regression coefficients b(i) of the HRR variable for section P4 at variable inclination angles and workings resistance

Similar dependencies were observed for the distribution of the regression coefficients of variable R2 (Fig. 8). This area has the maximum impact in the absence of a production slope and resistance R/100 = 0.01. In this case, $b(i) = 2.7$. However, this is lower than the influence of the L2 area with $b(i) = -3.68$. With an increase in resistance and the angle of inclination of the workings, the regression coefficient values decrease sharply.

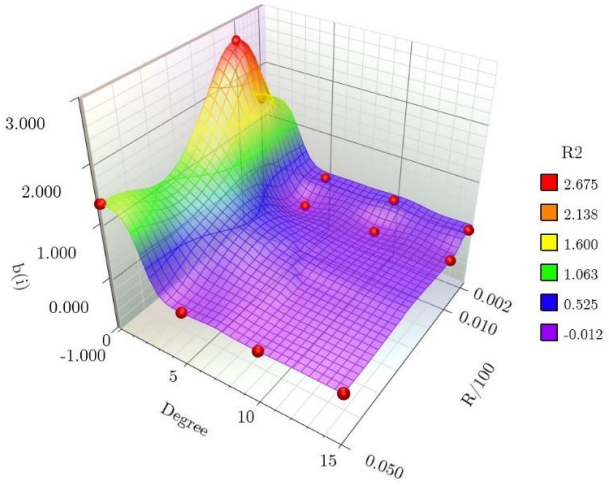

Figure 8. 3D surface plot of the multiple regression coefficients b(i) of variable R2 for section P4 at variable inclination angles and workings resistance

The surfaces of influence in the R3 area (Fig. 9) have two pronounced extremes. At degree = 0 and R/100 = 0.05, $b(i) = 0.9$ and at degree = 5 and R/100 = 0.002, $b(i) = -1.6$. At zero slope, $b(i)$ for R3 with R/100 = 0.01 was 0.79, and with R/100 = 0.002, it was 0.65. For these combinations of R/100 and degree, the air flows in the R3 section had the second degree of influence on the air flows in the P4 section after the L2 section. For sloped workings with resistances greater than 0.01, the influence of R3 on P4 is insignificant, and for small resistances (R/100 = 0.002), the regression coefficients have negative values. With an increase in airflow at R3, the airflow at the site decreased.

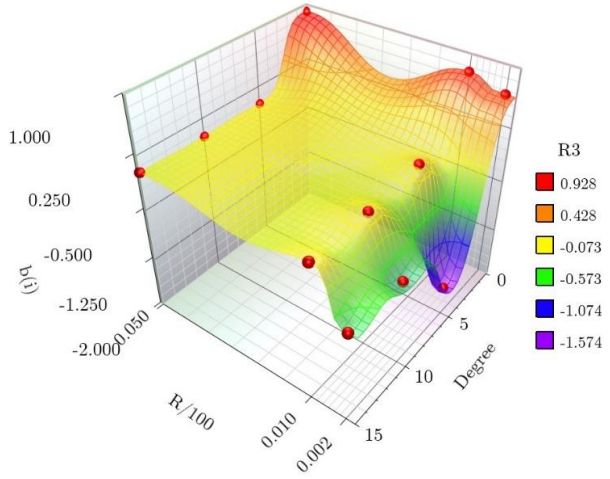

Figure 9. 3D surface plot of the multiple regression coefficients b(i) of the variable R3 for section P4 at variable inclination angles and workings resistance

The regression coefficients of the L2 plot (Fig. 10) were mostly negative. The exceptions are the two combinations for a slope of 5 and resistances of 0.002 and 0.05. The greatest influence of L2 was observed for horizontal work. In the slope work, the influence of L2 on P4 was low or very insignificant.

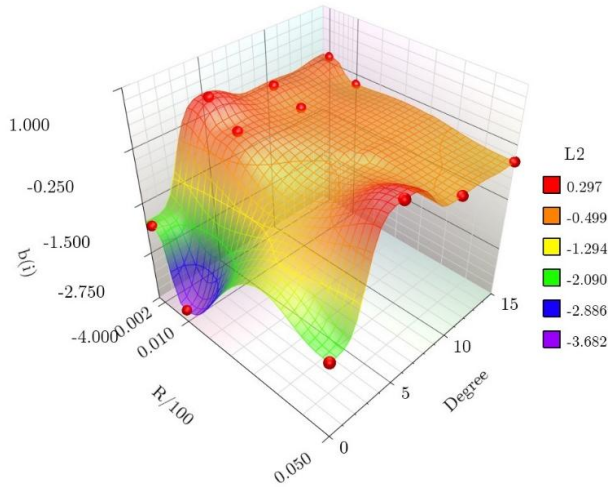

Figure 10. 3D surface plot of the multiple regression coefficients b(i) of the variable L2 for section P4 at variable inclination angles and workings resistance

The L3 plot (Fig. 11) is characterized by three extremes, all at degree = 5: a positive one at R/100 = 0.01 and two negative ones at linear resistances of 0.002 and 0.05, respectively.

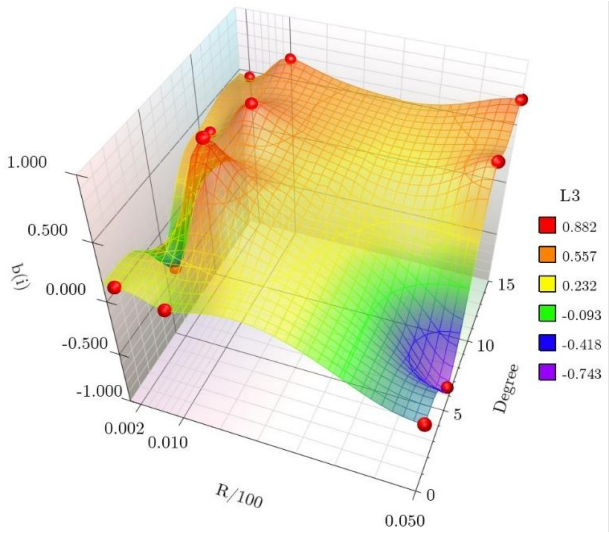

Figure 11. 3D surface plot of the multiple regression coefficients b(i) of the variable L3 for section P4 at variable inclination angles and workings resistance

In horizontal workings, the influence of L3 is much lower than that of other longitudinal sections, and in inclined workings, with resistances of R/100 = 0.002, the degree of influence of L3 ranks second, and with higher resistances, first.

We consider the effect of the adjacent sections and HRR on crosscut section P5. The summary 3D scatter plot (Fig. 12) shows that for most combinations of Degree and R/100, the main influence on P5 was exerted by the L3 and L4 sections. For the degree / (R/100) combinations of 5/0.002, 10/0.05, and 15/0.05, the main influential variable was R4, and the second most significant variable was R3. In the five combinations, the regression coefficients of L3 and L4 were very close. For degree = 0, at R/100 = 0.05, the main influential variable is L4, the second most significant variable is R4, and at 0.002 and 0.01, HRR is the main influential variable.

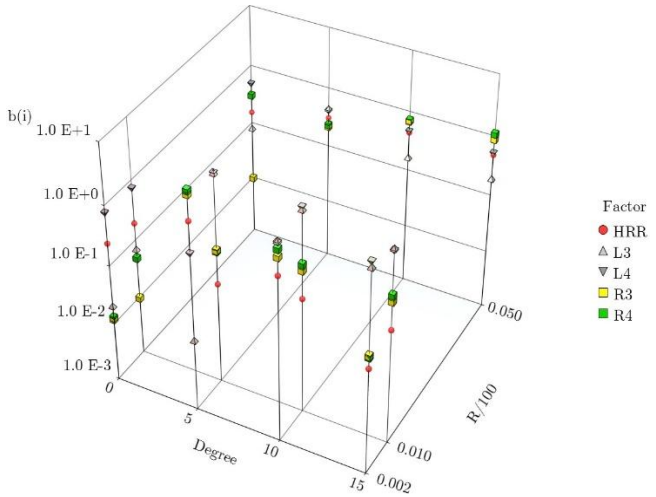

Figure 12. 3D scatter plot of the multiple regression coefficients b(i) of the variables R2, R3, L2, L3 HRR for section P5 at variable inclination angles and workings resistance

For section P5, compared with section P4, there was a noticeable increase in the influence of HRR (Fig. 13). This variable had the greatest impact when degree = 5 and R/100 = 0.002. For this combination, $b(i) = 1.61$. At a slope 5° and a resistance of 0.05, the regression coefficient has a negative value of -0.31.

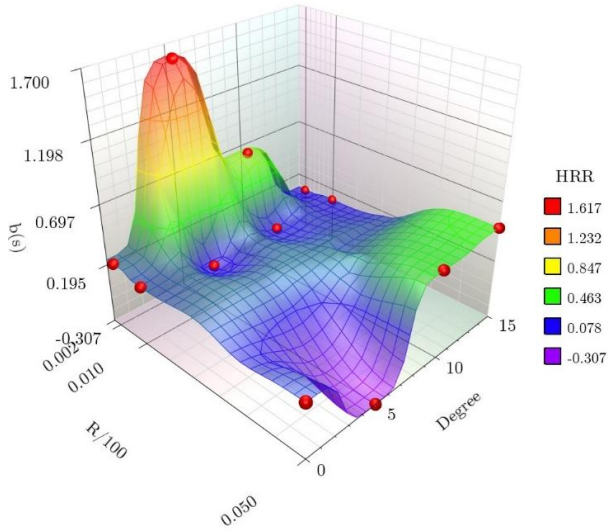

Figure 13. 3D surface plot of the multiple regression coefficients b(i) of the HRR variable for section P5 at variable inclination angles and workings resistance

For site P4, the surface of influence of variable R3 on site P5 is similar to the surface of influence of HRR (Fig. 14). This is due to the direct influence of HRR on the airflow in the area where the fire is located. The highest positive regression coefficient ($b(i) = 4.38$) was characteristic of the combination of degree = 2 and R/100 = 0.002. The largest negative regression coefficient ($b(i) = -0.219$) is for the combination of degree = 5 and R/100 = 0.052.

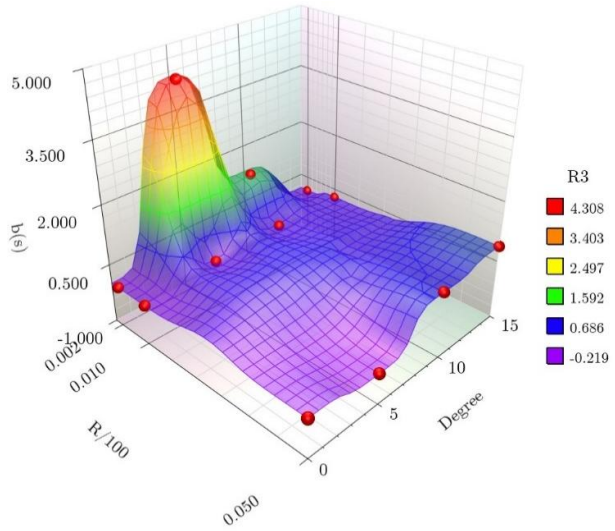

Figure 14. 3D surface plot of the multiple regression coefficients b(i) of the variable R3 for section P5 at variable inclination angles and workings resistance

The variable R4 is characterized by an extreme ($b(i) = -4.90$) for the combination of degree = 5 and R/100 = 0.002 (Fig. 15). With this combination, as well as with a resistance of 0.05 and slope 10 and 15°, the variable R4 ranked first in terms of its effect on air flows in section P5. With a resistance of 0.05 and slope 0 and 5°, the regression coefficient had positive values, whereas, in other combinations, it was negative.

The variable L3 is characterized by two negative extremes $b(i) = -3.6198$ at degree = 5 and R/100 = 0.01 and $b(i) = -2.8922$ at degree = 15 and R/100 = 0.002.

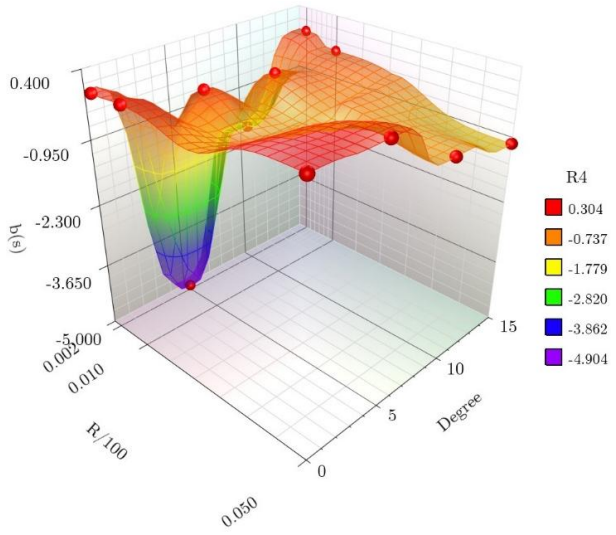

Figure 15. 3D surface plot of the multiple regression coefficients b(i) of the variable R4 for section P5 at variable inclination angles and workings resistance

There is also a positive extremum $b(i) = 0.4539$ at degree = 5 and R/100 = 0.05 (Fig. 16). Variables L3 and L4 significantly affected P4 in the inclined workings. The exceptions are the combination of resistance of 0.05 and inclination angle 10°and 15°, as well as resistance of 0.002 and inclination of 5°.

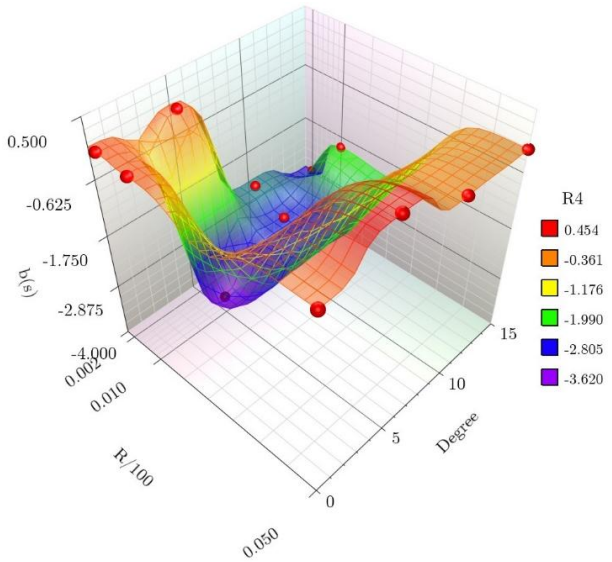

Figure 16. 3D surface plot of the multiple regression coefficients b(i) of the variable L3 for section P5 at variable inclination angles and workings resistance

The variable L4 was characterized by two extremes with positive values of the regression coefficients of 2.14 and 3.31 at a resistance of 0.002 and slope angle10° and 15°, respectively (Fig. 17). Another positive extremum with a regression coefficient of 3.41 was found at a resistance of 0.01 and an inclination angle of 5°. In general, the values of the regression coefficients for the variable L4 were positive; however, at a resistance of 0.05 and an inclination angle of 5°, the coefficient value became negative and equaled -0.39. For horizontal working, L4 was dominant in terms of its influence on P5.

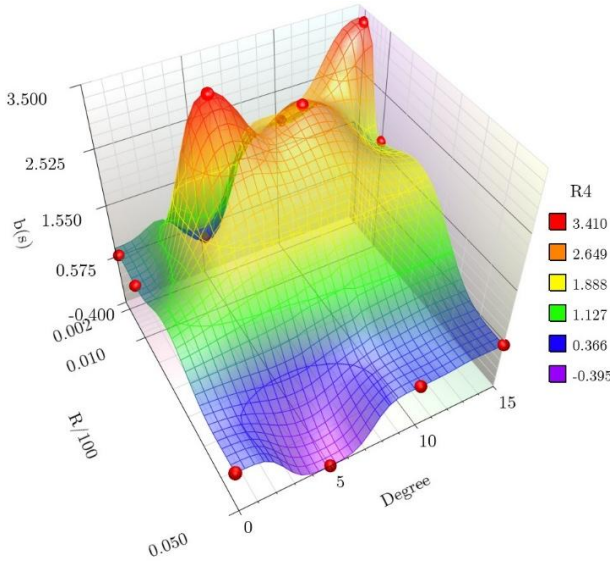

Figure 17. 3D surface plot of the multiple regression coefficients b(i) of the variable L4 for section P5 at variable inclination angles and workings resistance

The main variable L4 was also at an angle of inclination 10° and a resistance of 0.01, as well as at an angle 15° and a resistance of 0.002. The second most influential variable in P5, L4, has a slope 5° and resistances of 0.01 and 0.05, a slope 10° and resistance of 0.02, and a slope 15° and resistance of 0.01.

The results show that the crosscut section located immediately behind the section with the fire center is mainly influenced by the "cold" longitudinal sections located above and below and the "hot" section with the fire center. Simultaneously, an increase in the inclination angle, together with an increase in the resistance of the working face, increases the influence of the area with the fire center. In the case of a decrease in the inclination and resistance of the working face, the value of the "cold" adjacent workings increases.

The study found that the angle of inclination and linear resistance had a significant impact on the volume of airflow in mine workings, as evidenced by the negative correlation recorded in both the "hot" and "cold" zones. The positive correlation between the slope angle and airflow during fire growth emphasizes the importance of mine geometry in the design of ventilation schemes under difficult conditions.

The study [16] corroborates the relationship between the angle of inclination and airflow behavior during a fire. It has been demonstrated that the maximum impact of the Heat Release Rate (HRR) on both air and tunnel wall temperatures is most pronounced in horizontal tunnels. The authors assert that, in this scenario, the maximum excess temperature exhibits a linear dependence on the HRR raised to the power of 2/3. Conversely, when the fire source is situated in an inclined tunnel, the maximum excess temperature is influenced by the angle of inclination (3, 4 or 5%). As the inclination increases, the maximum excess temperature generally diminishes due to the intensified flow induced by buoyancy, although specific numerical results for each inclination are not provided. These findings align with our results concerning the dependence of the degree of HRR's impact on airflow characteristics on the tunnel's angle of inclination (Fig. 7).

The findings of research [17] indicate that an increase in both the inclination of the excavation and the HRR results in a rise in airflow velocity, thereby causing asymmetry. This phenomenon leads to the tilting of the smoke plume and the displacement of the maximum ceiling temperature towards the upper entrance of the excavation. These observations align with the relationships established in our study between Fire HRR, the temperature of the working zone walls, and the airflow in the longitudinal sections of the working area (Table 6). Study [17] highlights that asymmetric inflow alters the mechanisms of heat transfer: convection becomes predominant towards the upper end due to enhanced flow, while radiation is more significant near the fire source. Consequently, this results in uneven ceiling heating, with potential hot spots shifting upward. In Table 6 of our research, this is evidenced by a notable decrease in the correlation coefficient (from 0.908 to 0.502) between the factors *T* rock and R3 at the second stage of the fire.

The study [18] examines the influence of the inclination of the main tunnel line on the characteristics of smoke movement and the extent of smoke back-layering in a naturally ventilated branched tunnel with an inclined lower main line. The empirical equations derived in this research indicate a reduction in backflow values with increased resistance of the working. This results in enhanced stability of airflows, as corroborated by our findings, which demonstrate that increased resistance of the working contributes to reducing the variability of correlation coefficients between the flow rates in adjacent workings for inclination angles ranging from 5 to 15°.

The presence of corroborating evidence from independent studies conducted by different groups of authors underscores the reproducibility and reliability of the results, demonstrating that these findings are not idiosyncratic to a particular methodological approach.

A comprehensive analysis of the thermal characteristics of the fires in this study revealed a significant positive correlation between the rate of heat release and airflow in the "hot" sections. These results are consistent with those of Zhang and Li (2024) [2], but this study offers a more detailed explanation of how thermal processes affect airflow patterns. The identified interaction between the wall temperature and airflow at different stages of the fire emphasizes the need for further research in this area, particularly in the context of operational firefighting measures.

For the transverse section P5, located above the fire center, the extremes of the correlation coefficients for all the accepted variables were located in the zone corresponding to the minimum value of R/100 (R/100 = 0.002) and the angle of inclination of the working face of 5°. An increase in the angle of inclination of the working and/or an increase in the aerodynamic drag of the working significantly reduced the value of the correlation coefficients. The variables L3 and L4 (cold areas) were also characterized by additional extremes at the combination of R/100 = 0.05 and a working angle of 5°. In particular, the correlation coefficient for L4 was negative. This means that an increase in the airflow volume in the "cold" section, which is located above the transverse section P5, leads to a decrease in the airflow volume in section P5.

For the combination of all accepted variables and the cross-section P5, another characteristic zone with fewer extremes was the zone with degree = 10 and R/100 = 0.002. The combination of P4/R4 at slope angles of 5° or more had negative correlation coefficients. However, this indicates that the air flows of area P5 were fed by the flows of the area with the fire center R3. The areas R4-R6 located above create aerodynamic resistance to the air flows arising from the fire, so the air chooses the path of least resistance and passes through transverse area P5. The less air that passes through section R4, the more air passes through section P5, and vice versa. At low aerodynamic drags (R/100 = 0.002), an increase in the angle of inclination led to a decrease in the relationship between the air flows of R4 and P5. Conversely, at high aerodynamic drag (R/100 = 0.05), an increase in the angle of inclination increases this relationship.

For the transverse section P4, which is located below the fire center, the largest number of extremes of correlation coefficients for all accepted variables are in the zone with R/100 = 0.01 and a slope angle of 0°. Two smaller extremes were characteristic of degree = 0 and R/100 = 0.002 and R/100 = 0.05. The data obtained allow us to conclude that the air flows of the transverse section located immediately below the fire center (P4) are most closely related to the air flows of the "cold" longitudinal section (L2) located below the fire center. Moreover, the greatest interaction was observed at a zero angle of inclination of the working face. As the inclination angle increased, the primary interaction of the air flows in the P4 section occurred with the air flows of the L3 section located above it. The second most influential factor for section P4 was the air flow in the upstream "cold" longitudinal section L3. Moreover, whereas for the P4/L2 interaction, an increase in the airflow in L2 leads to a decrease in the flow in P4, for the P4/L3 combination, an increase in the flow in L3 leads to an increase in the flow in P4. In other words, at working face inclination angles of 5° or more, the L3 section supplied air to the P4 section.

In general, it can be noted that an increase in the resistance of the working face helps reduce the variability of the correlation coefficients for inclination angles in the range of 5°-15°. This observation is relevant for both the transverse workings located below (P4) and above (P5) the fire center. The standard deviations of the values of the correlation coefficients for P4 at R/100 = 0.002 and inclination angles of 5°, 10°, and 15° were 0.75, 0.44, and 0.42, respectively, and at R/100 = 0.05-0.39, 0.42, and 0.47, respectively. For P5, at R/100 = 0.002, these values are 3.35, 1.98, 2.2, and at R/100 = 0.05, 0.37, 0.57, and 0.77. Thus, it can be concluded that an increase in the total resistance contributes to the stabilization of airflow in inclined workings.

The distribution of airflow in mine workings is extremely important for ensuring safety. The stability of the airflow in P4, the area under the fire, combined with the instability in P5, highlights the complexity of airflow interaction in the mine environment. The use of complex methods, such as CFD modeling and correlation analysis, contributes to a deeper understanding of these dynamics. However, further research is required to improve existing ventilation systems and fire response methods.

The significance of the results obtained is extremely important, as they form the basis for the development of new risk management strategies and operational measures in the event of fires. Considering factors such as slope and resistance in the design of mine ventilation systems is key to effective emergency response. Thus, this study makes a significant contribution to mine safety by providing a practical basis for further research and development in this field.

4. Conclusions

This study analyzed the factors affecting airflow in mine workings through correlation analysis, focusing on the significance of linear resistance and angle of inclination in "hot" and "cold" areas relative to a fire center. Results show that:

There is a strong inverse relationship between linear resistance and airflow volume in the both "cold" and "hot" zones, especially in sections R2, L2, and L6. During fire growth, the airflow volume is significantly related to the angle of the working face. This relationship is much stronger in the hot zones, but less so in the cold zones.

During fire growth, there is a strong positive correlation between Fire HRR and airflow, especially in R2 in the "hot" sections and L2, L6 in the "cold" sections.

Wall temperature and airflow volume are significantly related at different stages of fire intensity, especially in the "hot" zones. Increasing the wall temperature increased the degree of this relationship in all areas except for L3, where the relationship increased without changing the wall temperature.

The airflow dynamics in the cross sections is related to the airflow dynamics in the longitudinal sections. Stable air flow is observed in section P4, which is located below the fire center, while section P5, which is located above the fire, is the most unstable.

The study used multiple regression analysis to evaluate the impact of various airflow variables in the P4 and P5 cross-sections. Key findings include:

At zero slope (degree = 0), a change in the airflow volume in the lower "cold" section L2 significantly increases the airflow in section P4, with the highest regression coefficient value recorded for low linear resistance (R/100 = 0.01).

At a five-degree slope, a greater change in airflow at section P4 occurs when airflow changes in the area with the fire center (R3) and in the "cold" zone (L3). Resistance and slope angles change the regression coefficients for each pair of factors.

Changing the Fire HRR has very little effect on the change in airflow volume in P4.

The change in airflow in section P5 at different combinations of inclination and resistance is particularly related to the changes in airflow in sections L3 and L4. The change in Fire HRR and the change in airflow in section P5 are significantly related at a face dip of five degrees. As in section P4, dip and resistance significantly affect the regression coefficients for each pair of factors.

The data obtained indicate that the fire center exerts the greatest influence on the airflow pattern of the nearest transverse section located above it. Conversely, the airflow pattern of the nearest transverse section situated below the fire center is more significantly affected by the airflow patterns of the nearest upper and lower "cold" sections.

Author contributions

Conceptualization: DB; Data curation: RM; Formal analysis: RM, SS; Funding acquisition: DB; Investigation: RM, SS, LY; Methodology: RM, LY, OP; Project administration: DB; Resources: OP; Software: SS; Supervision: DB; Validation: RM, OP; Visualization: SS; Writing – original draft: RM, SS, LY; Writing – review & editing: DB, RM, SS, LY. All authors have read and agreed to the published version of the manuscript.

Funding

This research received no external funding.

Conflicts of interest

The authors declare no conflict of interest.

Data availability statement

The original contributions presented in the study are included in the article, further inquiries can be directed to the corresponding author.

References

[1] Hodge, R.A., Ericsson, M., Löf, O., Löf, A., & Semkowich, P. (2022). The global mining industry: corporate profile, complexity, and change. *Mineral Economics*, *35*(3-4), 587-606. https://doi.org/10.1007/s13563-022-00343-1

[2] Zhang, M., & Li, Z. (2024). Experiments on a mine system subjected to ascensional airflow fire and countermeasures for mine fire control. *Fire*, *7*(7), 223. https://doi.org/10.3390/fire7070223

[3] Wang, J., & Wu, B. (2024). Thermal characterization analysis of pool fire affected by sealing in coal mine dead-end roadways: An experimental study. *Journal of Thermal Analysis and Calorimetry*, *149*, 12929-12945. https://doi.org/10.1007/s10973-024-13679-3

[4] Litwiniszyn, J. (1987). Remarks on the sign-changeable velocity of airflow in transverse sections of mine workings. *Mining Science and Technology*, *6*(1), 31-35. https://doi.org/10.1016/S0167-9031(87)90478-6

[5] Król, A., Szewczyński, K., Król, M., Koper, P., Bielawski, J., & Węgrzyński, W. (2024). Full-scale experimental, numerical, and theoretical research on the spatio-temporal evolution of the flow structure in longitudinal and semi-transversal ventilated tunnels. *Tunnelling and Underground Space Technology*, *147*, 105721. https://doi.org/10.1016/j.tust.2024.105721

[6] Jiang, L., & Xiao, M. (2022). Effect of tunnel slope on the critical velocity of densimetric plumes and fire plumes in ventilated tunnels. *Tunnelling and Underground Space Technology*, *123*, 104394. https://doi.org/10.1016/j.tust.2022.104394

[7] Wan, H., Gao, Z., Han, J., Ji, J., Ye, M., & Zhang, Y. (2019). A numerical study on smoke back-layering length and inlet air velocity of fires in an inclined tunnel under natural ventilation with a vertical shaft. *International Journal of Thermal Sciences*, *138*, 293-303. https://doi.org/10.1016/j.ijthermalsci.2019.01.004

[8] Yang, D., Guo, X., Jiang, L., & Du, T. (2024). Prediction model of buoyancy-driven flow rate in inclined tunnels with a localized buoyancy source: Emphasis on stratification effects. *Building and Environment*, *250*, 111165. https://doi.org/10.1016/j.buildenv.2024.111165

[9] Hu, D., Li, Z., Wang, H., Xu, H., & Miao, C. (2023). Smoke dispersion test and emergency control plan of fire in mine roadway during downward ventilation. *Scientific Reports*, *13*(1), 3683. https://doi.org/10.1038/s41598-023-30779-6

[10] Zhang, M., Li, Z., Li, T., Wang, H., Xu, H., & Yang, Z. (2021). Experiments of mine fire in ascending airflow and the mine fire control simulation. *Journal of China Coal Society*, *46*(S2), 785-792. https://doi.org/10.13225/j.cnki.jccs.2021.0873

[11] Brovko, D., Makareiko, R., Sakhno, S., Yanova, L., & Pischikova, O. (2024). Modeling the stability of air flows in inclined workings in case of fire. *Mining of Mineral Deposits*, *18*(3), 52-62. https://doi.org/10.33271/mining18.03.052

[12] Thi, H.N., & Van, Q.N. (2023). Numerical study on effects of airflow parameters on the air temperature the at mechanized longwall of Mongduong coal mine. *Inzynieria Mineralna*, *1*(2), 89-96. https://doi.org/10.29227/IM-2023-02-16

[13] Guo, L., Nie, W., Yin, S., Liu, Q., Hua, Y., Cheng, L., Cai, X., Xiu, Z., & Du, T. (2020). The dust diffusion modeling and determination of optimal airflow rate for removing the dust generated during mine tunneling. *Building and Environment*, *178*, 106846. https://doi.org/10.1016/j.buildenv.2020.106846

[14] Chen, D., Xie, J., Wang, Y., Sun, X., Du, H., & Li, G. (2023). CFD modeling of optimal airflow rates for safe production in isolated mining faces with high methane concentration and coal spontaneous combustion. *Journal of Cleaner Production*, *423*, 138835. https://doi.org/10.1016/j.jclepro.2023.138835

[15] Fetri, M., Shahabi, R.S., Namin, F.S., Zeyni, E.E., & Khereshki, M.H.K. (2023). Analysis of the impact of natural ventilation caused by excava-

tion of the waste passage on the ventilation network of Angouran mine. *International Journal of Mining and Geoengineering*, *57*(3), 231-240. https://doi.org/10.22059/IJMGE.2022.342133.594970

[16] Gong, L., Jiang, L., Li, S., Shen, N., Zhang, Y., & Sun, J. (2016). Theoretical and experimental study on longitudinal smoke temperature distribution in tunnel fires. *International Journal of Thermal Sciences*, *102*, 319-328. https://doi.org/10.1016/J.IJTHERMALSCI.2015.12.006

[17] Li, Y.Z., & Ingason, H. (2014). Position of maximum ceiling temperature in a tunnel fire. *Fire Technology*, *50*(4), 889-905. https://doi.org/10.1007/S10694-012-0309-2/METRICS

[18] Huang, Y., Liu, X., Dong, B., Zhong, H., Wang, B., & Dong, Q. (2023). Effect of inclined mainline on smoke backlayering length in a naturally branched tunnel fire. *Tunnelling and Underground Space Technology*, *134*, 104985. https://doi.org/10.1016/J.TUST.2023.104985

Чисельне дослідження впливу кута нахилу та опору гірничих виробок на формування повітряних потоків під час пожежі

Д. Бровко, Р. Макарейко, С. Сахно, Л. Янова, О. Пищикова

Мета. Метою даного дослідження було вивчення впливу кута нахилу та аеродинамічного опору гірничих виробок на динаміку повітряних потоків під час пожежі.

Методика. Для аналізу динаміки повітряних потоків під час пожежі було застосовано модель, засновану на вентиляційній мережі кар'єру "АрселорМіттал Кривий Ріг" з кутом нахилу 15 градусів. Повітряний потік під час пожежі моделювався за допомогою програми Ventsim. Для виявлення впливу кута нахилу виробки та опору на характер повітряного потоку було використано кореляційний та множинний регресійний аналізи.

Результати. Кореляційний аналіз виявив значний негативний зв'язок між лінійним опором і об'ємом повітряного потоку в "холодних" і "гарячих" зонах. Кут нахилу та лінійний опір по-різному впливають на об'єм повітряного потоку залежно від розташування ділянки відносно центру пожежі. Основним фактором, що впливає на витрату повітря в поздовжніх перерізах, є лінійний опір. Вплив кута нахилу був найбільш вираженим у "гарячих" зонах. Результати свідчать, що на поперечний переріз, розташований безпосередньо за перерізом з осередком пожежі, в основному впливають "холодні" поздовжні перерізи, розташовані вище і нижче, а також "гарячий" переріз з осередком пожежі. Зі збільшенням кута нахилу та опору очисного вибою зростає вплив ділянки з осередком пожежі. У разі зменшення кута нахилу і опору очисного вибою значення "холодних" прилеглих виробок зростає.

Наукова новизна. У даній роботі представлено новий аналіз динаміки повітряних потоків у похилих гірничих виробках, зокрема під час пожеж. Дослідження сприяє кращому розумінню механізмів зміни напрямку струменя і поширення продуктів горіння під час пожеж у похилих виробках.

Практична значимість. Результати дослідження дозволяють прогнозувати виникнення пожеж, визначати зони, найбільш схильні до загоряння, та формувати оптимальні стратегії гасіння пожеж у конкретних умовах.

Ключові слова: *підземна пожежа, гірнича безпека, вентиляційна мережа, видобуток корисних копалин, обчислювальна гідрогазодинаміка*

Publisher's note

All claims expressed in this manuscript are solely those of the authors and do not necessarily represent those of their affiliated organizations, or those of the publisher, the editors and the reviewers.